Journal of Ceramic Processing Research. Vol. 11, No. 6, pp. 752~759 (2010)

J O U R N A L O F
Ceramic Processing Research

Rheological and wall slip properties of kaolinite-silicon oil pastes during extrusion

Zürriye Yilmaz, Mehmet Dogan* and Mahir Alkan
Balikesir University Faculty of Science and Literature Department of Chemistry 10145 Cagis-Balikesir/TURKEY

The rheological behavior of pastes was characterized by employing capillary flow. The wall slip properties of pastes are very significant in the extrusion process. All pastes were found to exhibit non-Newtonian, pseudoplastic, shear thinning behavior under all experimental conditions in a wide apparent shear rate range of 1-4000 1/s. It was found that the corrected shear stress values increased with an increase in the solid:liquid ratio and particle size, and with a decrease in temperature at above 100 kPa. The results confirm that the computed shear stress depends upon both the diameter and the length of the capillary tube; and also show that the influence of the wall slip is significant and that the wall slip velocities increase with an increase in shear stress. The Mooney method was applied to examine the nature of the shear flow. It was concluded that the slip effects dominate the flow of kaolinite-silicon oil pastes at a high shear stress (above 100 kPa) and true flow and deformation characteristics of the pastes may be overshadowed by slip at the walls. The contribution of the slip of the paste at the wall to the volumetric flow rate in capillary flow was found to increase with an increase in temperature, particle size and amount of solid.

Key words: Kaolinite, silicon oil, paste, wall slip analysis, Mooney method.

Introduction

Semi-solid pastes are concentrated suspensions of particles suspended in a flux-vehicle medium [1]. The rheological properties of suspensions of solid particles in polymeric matrices are important in analyzing the processing of such materials, which are encountered in various industries. The rheological behavior of these composite systems depends on the particle shape, size and size distribution, volume fraction of particles, particle-particle and particle-matrix interactions, matrix rheology, and measurement conditions such as the temperature and shear rate. Dilute suspensions of small particles in Newtonian fluids also behave as Newtonian fluids in most cases. However, the situation for concentrated suspensions is more difficult to analyze from a theoretical perspective compared to dilute suspensions [2]. The characterization of these suspensions is firstly complicated by structural changes, which may occur during the characterization, and secondly by possible slip at the walls of the capillary dies [3].

Extrusion processes of pastes are frequently used in the ceramic industry. In order to model and/or optimize paste extrusion, one must have knowledge of the material's flow properties. The flow properties of the pastes; particularly, the flow behavior of the wall-adjacent layers, i.e. the wall slip properties are very significant in extrusion processes [4]. The flow of paste-like materials invariably involves interactions at the interface between the material and the processing engine wall [5]. Understanding the material's wall slip behavior inside a capillary or an extrusion die is particularly important, both for modeling the process and attaining good practical results [4]. Due to migration of the liquid-phase at the interface between the paste and the engine wall, this creates a liquid phase rich layer at the interface, which might typically have a thickness of one particle diameter [3, 6-10]. This interface layer may act as a lubricant and allow the paste to slip against the wall. The material flow response is highly dependent upon the interfacial characteristics of the boundary; therefore, the nature of the boundary is very important in the paste processing operation [5]. This wall influence, which generally reduces the shear strength of the particle network, extends from the wall to a distance of approximately a few particle diameters. At sufficiently high shear loadings the particle structure collapses in the layer of paste near the wall, causing formation of a thin film, which allows the paste to flow via slip along the wall [4]. A study of the effect of wall slip in viscosity measurements and in the industrial processing of concentrated suspensions has been reported for a range of applications such as die extrusion and injection modeling of metal or ceramic pastes [1]. The relative slip velocity changes with increase in temperature. The changes in the viscosity of the fluid phase, extrudate velocity and shear stress have an effect on the slip behavior. In general, the behavior of the particulate pastes during extrusion depends on: 1. the amount and rheological properties of liquid phase, 2. the interference between particles, 3. the extrusion conditions, and 4. the time scale of the experiments [11].

Various methods have been used to examine the rheological properties of ceramic pastes. The wall slip behavior of pastes during extrusion can be characterized via capillary rheometry. Capillary extrusion flow has been very often utilized for a wide variety of paste-like materials in an

*Corresponding author:
Tel : +90-266-612-1000
Fax: +90-266-612-1215
E-mail: mdogan@balikesir.edu.tr

attempt to characterize their bulk intrinsic rheology as well as their wall interface boundary conditions. The commonly used classical measurement methods are the Mooney method, a color making method and a twin capillary method [4]. The purpose of this study has investigated the wall slip properties of kaolinite-silicon oil pastes prepared under different conditions according to the Mooney method. In previous investigation, some rheological properties of both kaolinite and silicon oil had been studied by different researchers. Zhao *et al*. investigated the synthesis and electrorheological activity of a modified kaolinite/carboxymethyl starch hybrid nanocomposite [12]; Neto and Moreno the rheological behavior of kaolin/talc/alumina suspensions for manufacturing cordierite foams [13]; Dai *et al*. the thixotropy behavior of Mg-Al-layered double hydroxides/kaolinite dispersion [14]; Baird and Walz the effects of added nanoparticles on aqueous kaolinite suspensions [15]; Zhang *et al*. the rheological properties of clay suspensions in silicone fluid [16]; Zhang *et al*. the effect of both surface modification of kaolin and the end groups of PDMS on dispersing kaolin into PDMS melts and characterized how kaolin particles affect the properties of PDMS and the resulting composites [17]; Swallow the viscosity properties of polydimethylsiloxane gum [18]; Paquien *et al*. the rheological properties of fumed silica-polydimethylsiloxane suspensions [19].

A theory of capillary flow and analysis of wall slip

The usual method to investigate the flow functions of fluids is the measurement of the pressure loss Δp along a capillary. The apparent values of the shear rate at the die wall, $\dot{\gamma}_w$, the wall shear stress, τ_w, and shear viscosity during the extrusion of a sample material through a capillary die, are given by Eqs. (1)-(3), respectively:

$$\dot{\gamma}_w = \frac{4V}{\pi R^3} \quad \text{for Newtonian fluids} \tag{1a}$$

$$\dot{\gamma}_w = \frac{4Q}{\pi R^3}\left(\frac{3n+1}{4n}\right) \quad \text{for non-Newtonian fluids} \tag{1b}$$

$$\tau_w = \frac{\Delta p \cdot R}{2L} \tag{2}$$

$$\eta_a = \frac{\tau_w}{\dot{\gamma}_w} \tag{3}$$

where R is the capillary radius; L is the length of the capillary; Δp is the total pressure drop over the capillary. The wall shear stress is a function of the wall shear rate in the fluid. For a given volume rate V, the shear rate depends only on the radius of the capillary, in which $n = [d(\log\tau)]/[d(\log\gamma)]$. Equation (1a) is valid for Newtonian fluids and Equation (1b) for non-Newtonian fluids. The boundary condition for both Eqs. (1a) and (2) is adhesion to the wall [4, 20].

A Mooney analysis was performed on end-corrected data to obtain the wall slip velocity (V_{slip}). In this procedure, the apparent shear rate is assumed to be a sum of the corrected shear flow. The observed flow rate, Q_{app}, may be intuitively considered to be composed of two nominally separate flow contributions:

$$Q_{app} = Q_{true} + Q_{slip} \tag{4}$$

The first term on the right hand side is the intrinsic internal shear flow rate, Q_{true}, and the second term is the separate contribution provided entirely by the slip at the wall. Eq. (4) may be converted to Eqs. (5) and (6):

$$\frac{\dot{\gamma}_w \pi R^3}{4} = \frac{\dot{\gamma}_{true} \pi R^3}{4} + V_{slip} \pi R^2 \tag{5}$$

$$\dot{\gamma} = \dot{\gamma}_{true} + \frac{4V_{slip}}{R} \tag{6}$$

where $\dot{\gamma}_w$ and $\dot{\gamma}_{true}$ are the observed (apparent) and true shear rate, and V_{slip} is the wall slip velocity. The first term on the right hand side of Eq. (6) describes the part of the nominal Newtonian shear rate that depends only upon the shear stress at the wall, as opposed to the capillary diameter. The parameter V_{slip} in Eq. (6) may be expressed as:

$$V_{slip} = f(\tau_B) \tag{7}$$

where $f(\tau_B)$ is a function of the Bagley corrected wall shear stress (τ_B). A plot of $\dot{\gamma}_w$ versus (1/R) for Eq. (6) should be a straight line. $\dot{\gamma}_{true}$ is the ordinate value at (1/R) = 0, and the slip velocity $4V_{slip}$ is the slope of line [4, 6, 21].

Material and Methods

Materials

Silicon oil AK 1 000 000 was supplied by Wacker-Chemie GmbH. Kaolinite was obtained from Kale Maden from Balikesir in Turkey. The model pastes consisted of kaolinite particles with a mean diameter 0-25 μm, and silicon oil with a molecular weight MW 200,000 and limiting viscosity at zero shear rate η_0 1170 Pas.

Paste preparations

The paste was prepared from the kaolinite and silicon oil AK 1 000 000. Firstly, kaolinite powders were mixed in a kneader (IKA HKD-T0,6 Kneader) and, then the liquid phase was added. The silicon oil based paste was mixed batchwise in the kneader for four hours to achieve better homogenization. At various intervals during the mixing, the process was stopped and paste was detached from the blades of the mixture using a spatula. The prepared paste was stored in sealed containers at room temperature. The formulation of the concentrated suspensions, the investigated parameters and the dimensions of capillary dies are shown in Table 1. The IKA-high-efficiency laboratory kneader is suitable for processing non- flowable, highly-viscous media. The uniform mixing is based on intensive processing

by means of wide-bladed kneading elements. The kneading medium is moved within the trough both horizontally and vertically. Additional media quantities may be added during the kneading operation. The complex layout of the blades and chamber can be seen in Fig. 1. The double-walled kneading chamber allows cooling or heating of the product. The product temperature may be measured directly behind the kneading blades [22, 23].

Table 1. Parameters investigated in the experiments

Particle sizes (μm)	Solid : liquid ratio (g : g)	Temperature (°C)	Die dimensione [L (mm)/D (mm)]
0-25 25-50	70 : 30	25	8/0.5;16/1;32/2
0-25	70 : 30 75 : 25	25	8/0.5;16/1;32/2
0-25	70 : 30	25 50 75	8/0.5;16/1;32/2

Rheological measurements

In this study, the rheological measurements were performed with a high pressure capillary rheometer (RH10 series, Rosand, Malvern) equipped with a computer for data acquisition. The pressure sensor of the capillary rheometer was located at the capillary entrance. Fig. 2 shows a cross-section of such a rheometer with barrel diameter D_0, die diameter D and die length L. The barrel could be fitted with different orifice and capillary dies; an orifice is a capillary of negligible length. The arrangement used consisted of orifices and capillaries of diameters ranging from 0.5-2.0 mm. The lengths of capillaries were 8, 16 and 32 mm. The barrel of the extruder was completely filled with the paste before every experiment. The ram forces paste to flow with a volumetric rate from the barrel into the die land. Capillary and orifice dies with different sizes were attached to the bottom of the barrel and the ram was moved downward by moving the top cross head of machine. All pastes were extruded from the capillary rheometer at wide shear rate ranges. The apparent shear viscosity and shear stress of pastes as a function of shear rate were measured [22, 23].

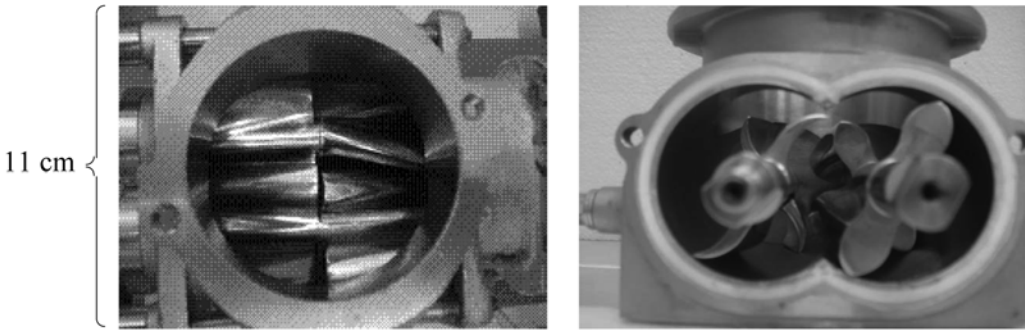

Fig. 1. Mixing blades and chamber for Ika Kneader MKD 0.6-H60.

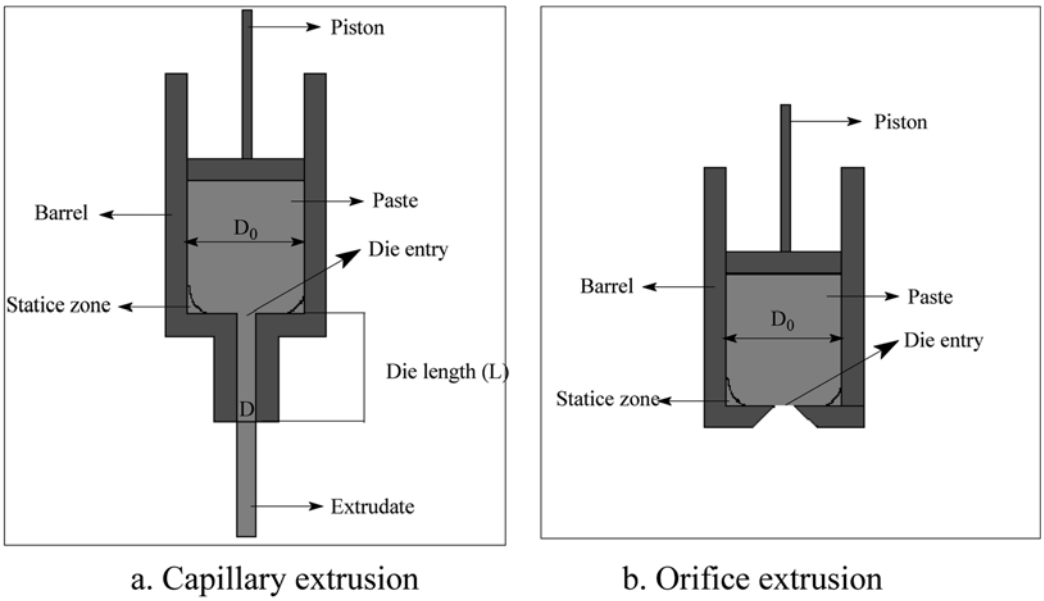

Fig. 2. Schematic representation of the cross-section of the basic elements of the capillary rheometer apparatus.

Results and Discussion

The twin capillary is a parallel connection of capillary and orifice dies as seen from Fig. 2. Figs. 3-5 show the end effect corrected shear stress versus the apparent shear rate behavior of the pastes with the series of capillaries that have a length over diameter (L/D) ratio of 16. It can be seen that all pastes studied show a dependence on the die diameter, suggesting a contribution of wall slip. This dependence is strongly influenced by solid:liquid ratio, particle size and temperature. The flow behavior of semi-solid materials under an applied stress classifies them as Newtonian or non-Newtonian, a classification that is based on their stress-strain relationship. The majority of the pastes do not show Newtonian flow behavior. Newtonian fluids have a straight line relationship between shear stress and shear rate with a zero intercept. For a non-Newtonian fluid the viscosity or shear stress is a function of the shear rate, meaning that for an applied shear rate the corresponding shear stress remains constant provided the shear rate has not changed [23, 24]. As seen from Figs. 3-5, flow plots of shear stress versus the apparent shear rate do not exhibit a linear relationship. In this case, it can be said that paste exhibits non-Newtonian flow behavior.

A non-Newtonian fluid is a fluid in which the viscosity changes with the applied strain rate. The viscosity of a fluid is affected by the binding between molecules that make up the solution or the relationship between the solvent and solute, both factors which are affected by solution concentration or temperature. Figs. 6, 7 and 8 shows the log-log plots of the shear viscosity against shear rate data for solid:liquid ratios, particle sizes and temperatures using different capillary dies. All of the samples have showed shear thinning behavior. This can be caused by either the alingment of kaolinite plates along the shear direction, if they are well-stabilized, or breakup of aggregates if they are floculated. As the kaolinite content is increased, pastes have a higher shear viscosity as expected due to the higher modules for the same surface treatment. This is ascribed to stronger particle interactions in the pastes. When external energy is supplied by heating to increase the temperature, it increases the energy of the molecules. The decrease in viscosity can be attributed to the increase in intermolecular distances, because of the thermal expansion caused by the increase in temperature [25]. Moreover, increasing the temperature softened the granules and the stresses imposed on them were large enough for deformation and flow. These figures also confirmed that all pastes in the shear rate ranges studied showed a pseudoplastic-shear thinning behavior [26]. A pseudoplastic material is one in which viscosity decreases with an increase in the shear rate. Pseudoplastic, or shear-thinning fluids have a lower shear viscosity

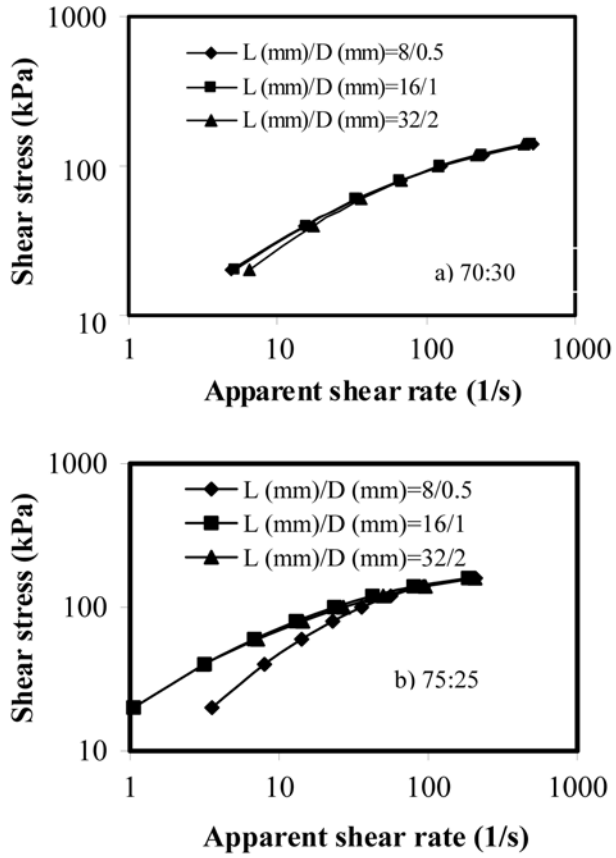

Fig. 3. Plots of shear stress versus apparent shear rate depending on the solid:liquid ratio.

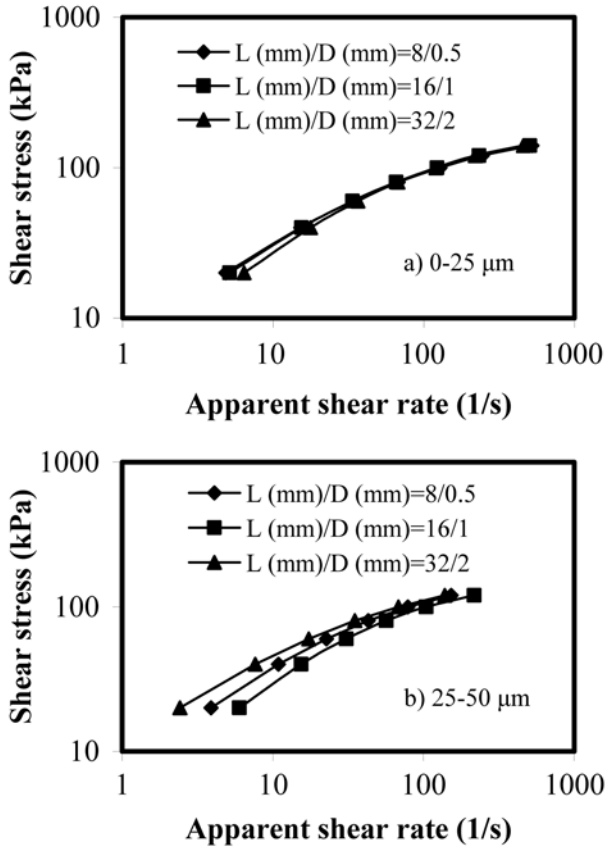

Fig. 4. Plots of shear stress versus apparent shear rate depending on the particle size.

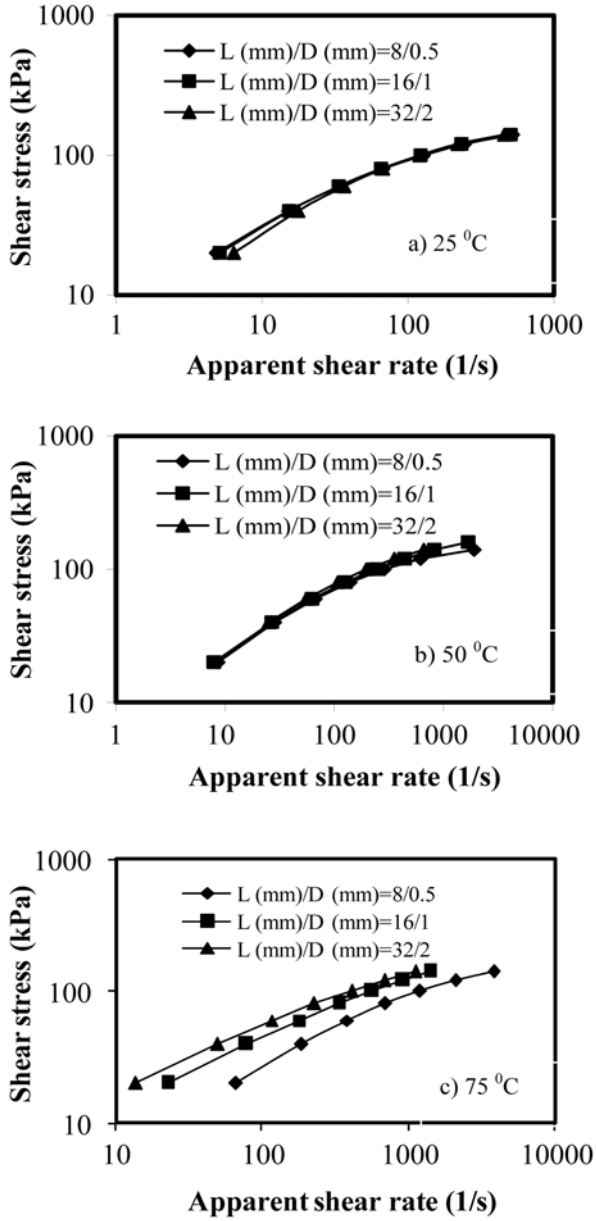

Fig. 5. Plots of shear stress versus apparent shear rate depending on the temperature.

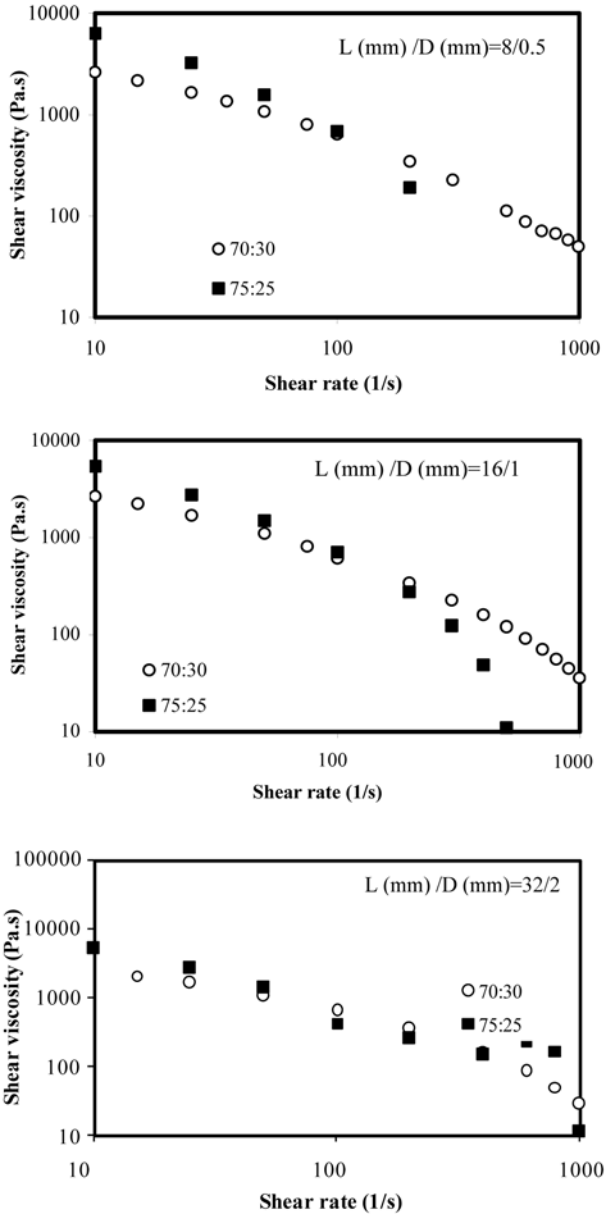

Fig. 6. Log-log plots of shear rate versus shear viscosity as a function of solid:liquid ratio.

at higher shear rates [27]. Again, these plots are commonly used to identify the existence of wall slip [28].

The shear stress in the pastes during capillary flow changes systematically when the amounts of liquid or solid are altered. Figs. 3(a) and (b) show the plots of corrected shear stress versus apparent shear rate as a function of the amount of solid or liquid. The corrected shear stress has increased with an increase in the amount of solid. At the low apparent shear rate region for Fig. 3(b), the curves do not overlap with each other, which may be due to wall slip. As seen from Fig. 4 for particle size, in the low apparent shear rate, the corrected shear stress increases with the increasing apparent shear rate, but at the high apparent shear rate regions the slope was lower than that at the low apparent shear rate region. This is typical for a material exhibiting a shear thinning phenomenon [28]. However, the corrected shear stress values obtained employing various capillaries with the same L/D ratio but with different diameters and lengths do not overlap with an increase in the apparent shear rate (Fig. 4(b)) when the values in the ranges of 0-25 μm overlapped with each other. This indicated the existence of pressure effects on the shear stress and end effects, which became more significant at higher barrel pressure. The fact that the curves at large particle sizes do not overlap with each other indicates that wall slip has taken place. Fig. 5 depicts the apparent flow curves of the paste for the dies with the same *L/D* ratios as dependent on the temperature. At a higher temperature, the shear stress (and hence, shear viscosity) was lower than those values obtained at lower temperatures as seen from Fig. 5.

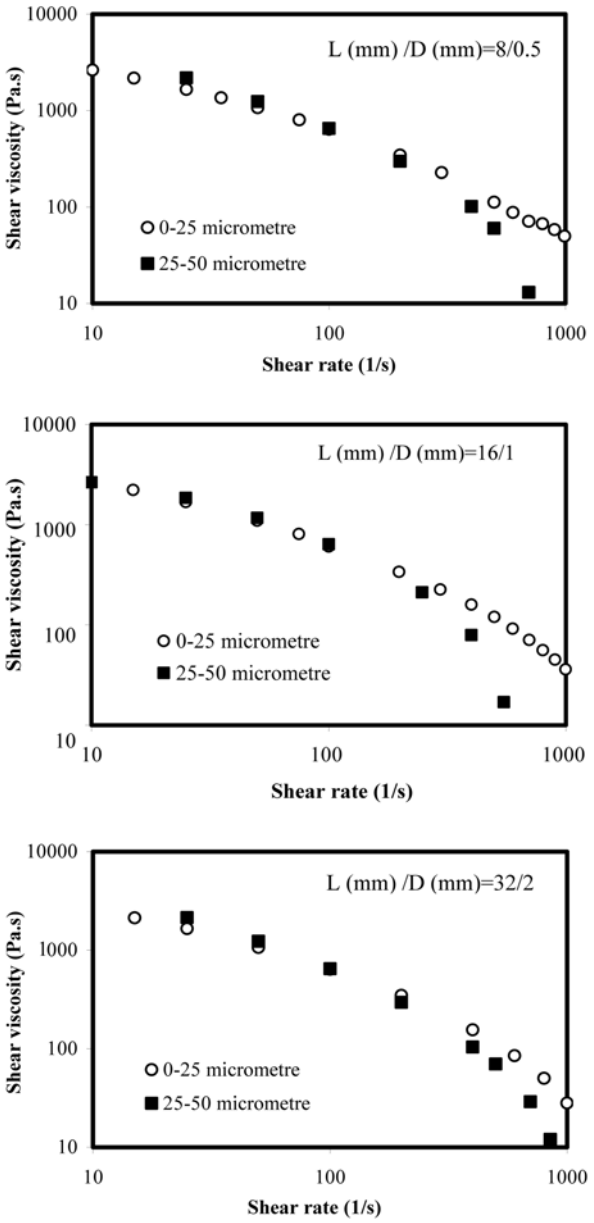

Fig. 7. Log-log plots of shear rate versus shear viscosity as a function of particle size.

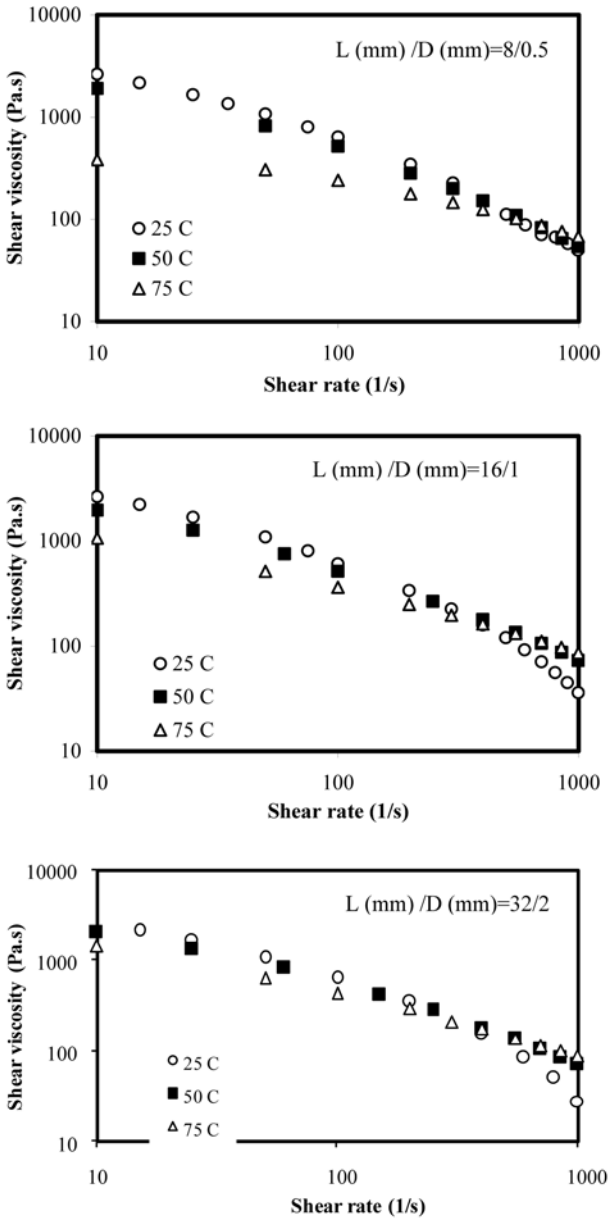

Fig. 8. Log-log plots of shear rate versus shear viscosity as a function of temperature.

The Mooney method for wall slip analysis was given by equation [6]. For the experimental determination of the wall slip velocity, it is necessary to measure the volume flow with capillaries of the same length-to-diameter (*L*/*D*) ratios at the same shear stress. A plot of the apparent shear rate versus 1/*R* at constant τ_w values should result in straight lines with slopes equal to $4V_s$ and intercepts equal to $\dot{\gamma}_{true}$ provided that the Mooney analysis is correct (Figures not shown) [3]. The wall slip behavior of a paste, characterized in terms of the plots of the slip velocity versus the wall shear stress, can be employed, not only for correcting the rheological data for the wall slip but can also be utilized in the simulation of the extrusion flows [21]. The slip velocity values, obtained from the capillary flow experiments, are plotted against the wall shear stress values as seen from Figs. 9-11. As seen from Figs. 9-11, V_{slip} values for all paste samples have increased at high shear stress values. If there is no slip flow at the wall, the rheological models measured in the same L/D ratio are the same for the same paste. From Figs. 3-5, it can be seen that the rheological models measured in different diameter sizes are generally different. The reason is just the slip phenomena of paste flowing in dies, which result in the existence of different rheological models for the same paste. Such flow instabilities observed in the capillary flows of concentrated suspensions typically occur in the relatively low wall shear stress range [29]. This is a result of a phase migration occurring in a paste showing a non-Newtoinan property under increasing shear stress. This phase migration becomes clearer with decreasing viscosity when the shear

stress increases. The change in slip velocity indicates that the surface layer properties rely on the amount of solid or liquid. All pastes depending on the solid:liquid ratio show low wall slip velocity in the shear stress range of 0-100 kPa, but wall slip velocity has significantly increased at above 100 kPa (Fig. 9). This may be a result of phase separation for pastes. To investigate the effect of particle size on wall slip velocity, the volume fraction was kept constant at 70 : 30 of the maximum volume fraction during the experiments. As seen from Fig. 10, as the particle size increases, the wall slip velocity values are low and the wall slip velocity has not significantly changed until a shear stress value is 100 kPa. But at high shear stress values above 100 kPa as seen from Fig. 10, the wall slip velocity increases markedly for all particle sizes. This indicates that the shear stress values of process conditions of pastes are lower than 100 kPa. Since the kinetic energy of molecules increases with temperature, the interaction between the kaolinite and silicone oil reduces and phase migration can occur more easily. The relationship between shear stress and V_{slip} with increasing temperature is shown in Fig. 11, indicating that wall slip has a significant contribution to the flow of the paste through the capillary die. Again, Fig. 11 shows that the wall slip velocity changes with temperature.

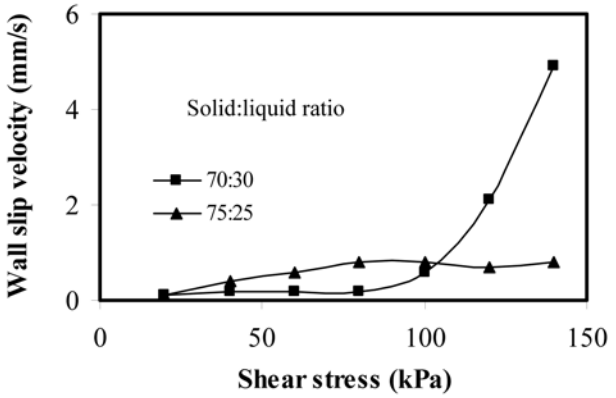

Fig. 9. Plots of wall slip velocity versus shear stress depending on the solid:liquid ratio.

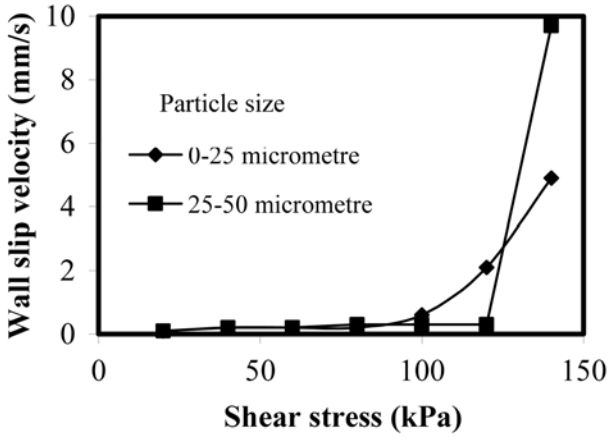

Fig. 10. Plots of wall slip velocity versus shear stress depending on the particle size.

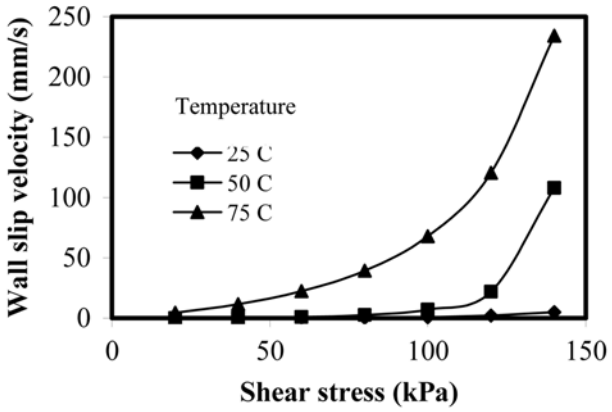

Fig. 11. Plots of wall slip velocity versus shear stress depending on the temperature.

Conclusions

The flow behavior of concentrated kaolinite-silicon oil pastes was characterized employing a capillary rheometer. The all pastes prepared behave as non-Newtonian, pseudoplastic, shear thinning fluids. The flow of concentrated pastes was found to be strongly affected by slip at the wall at a high shear stress. The use of the Mooney method to calculate the wall slip velocity was found to be suitable for interpreting the rheological behavior of the paste under investigation, as the paste material flowed principally by a slip process at the walls of the capillary. For most useful ceramic formulations the occurrence of wall slip will always be a major concern in the analysis of data or the application of a particular processing operation in practice. The paste system used in the study was deduced to be flowing during capillary extrusion predominantly by a slip process at the walls of the capillary.

Acknowledgements

The authors gratefully acknowledge the financial support of TUBITAK (TBAG 106T539).

References

1. N.N. Ekere, D. He and L. Cai, IEEE Transactions on Components and Packing Technologies. 24[3] (2001) 468-473.
2. S.A. Gulmus and U. Yilmazer, Journal of Applied Polymer Science. 98 (2005) 439-448.
3. U. Yilmazer and D.M. Kalyon, Journal of Rheology. 33[8] (1989) 1197-1212.
4. J. Graczyk, H. Buggisch and S. Güner, Chemical Engineering Technology. 24[5] (2001) 489-491.
5. A.U. Khan, B.J. Briscoe and P.F. Luckham, Journal of the European Ceramic Society. 21 (2001) 483-491.
6. M. Mooney, Journal of Rheology. 2 (1931) 210-222.
7. Y. Cohen and A.B. Metzner, Journal of Rheology. 29 (1985) 67-101.
8. H.A. Barnes, J. Non-Newtonian Fluid Mech. 56 (1995) 221-251.

9. R.J. Huzzard and S. Blackburn, Powder Technol. 97 (1998) 118-123.
10. D. Leighton and A. Acrivos, J. Fluid Mech. 181 (1987) 415-439.
11. J.J. Benbow, S. Blackburn and H. Mills, Journal of Materials Science. 33 (1998) 5827-5833.
12. X. Zhao, B. Wang and J. Li, Journal of Applied Polymer Science. 108 (2008) 2833-2839.
13. J.B.R. Neto and R. Moreno, Applied Clay Science. 37 (2007) 157-166.
14. X.N. Dai, W.G. Hou, H.D. Duan and P. Ni, Colloids and Surfaces A: Physicochem. Eng. Aspects. 295 (2007) 139-145.
15. J.C. Baird and J.Y. Walz, Journal of Colloid and Interface Science. 306 (2007) 411-420.
16. L-M. Zhang, C. Jahns, B.S. Hsiao and B. Chu, Journal of Colloid and Interface Science. 266 (2003) 339-345.
17. Y. Zhang, D.I. Gittins, D. Skuse, T. Cosgrove and J.S. van Duijneveldt, Langmuir. 24 (2008) 12032-12039.
18. F.E. Swallow, Journal of Applied Polymer Science. 84 (2002) 2533-2540.
19. J-N. Paquien, J. Galy, J.F. Gerard and A. Pouchelon, Colloids and Surfaces A: Physicochem. Eng. Aspects. 260 (2005) 165-172.
20. M. Fujiyama and H. Inata, Journal of Applied Polymer Science. 84 (2002) 2111-2119.
21. D.M. Kalyon, P. Yaras, B. Aral and U. Yilmazer, Journal of Rheology. 37[1] (1993) 35-53.
22. M. Dogan, J. Graczyk and H. Buggisch, Wissenschaftliche Abschlussberichte 38. Internationales Seminar, Universität Karlsruhe, Karlsruhe, GERMANY (2003).
23. M. Dogan, Z. Yilmaz and M. Alkan, Ind. Eng. Chem. Res. 47 (2008) 8218-8227.
24. S.N. Bhattacharya, Rheology: fundamentals and measurements. Australia: Royal Melbourne Institute of Technology (1997).
25. D.T. Constenla, J.E. Lozano and G.H. Crapiste, Journal of Food Science. 54 (1989) 663-668.
26. S.M.A. Razavi, M.B.H. Najafi and Z. Alaee, Food Hydrocolloids. 21 (2007) 198-202.
27. T.G. Mezger, The Rheology Handbook. Vincentz Network (2006).
28. J-C. Huang and Z. Tao, Journal of Applied Polymer Science. 87 (2003) 1587-1594.
29. U. Yilmazer, C.G. Gogos and D.M. Kalyon, Polym. Comp. 10 (1989) 242-248.